

Representing Roots on the Basis of Reeb Graphs in Plant Phenotyping

Ines Janusch¹, Walter G. Kropatsch¹, Wolfgang Busch², and Daniela Ristova²

¹ Vienna University of Technology
Institute of Computer Graphics and Algorithms
Pattern Recognition and Image Processing Group
Vienna, Austria

{ines, krw}@prip.tuwien.ac.at

² Gregor Mendel Institute of Molecular Plant Biology
Austrian Academy of Sciences
Vienna, Austria

{wolfgang.busch, daniela.ristova}@gmi.oeaw.ac.at

Abstract. This paper presents a new representation for root images based on Reeb graphs. The representation proposed captures lengths and distances in root structures as well as locations of branches, numbers of lateral roots and the locations of the root tips. An analysis of root images using Reeb graphs is presented and results are compared to ground truth measurements. This paper shows, that the Reeb graph based approach not only captures the characteristics needed for phenotyping of plants, but it also provides a solution to the problem of overlapping roots in the images. Using a Reeb graph based representation, such overlaps can be directly detected without further analysis, during the computation of the graph.

Keywords: Root Representation, Root Structure Analysis, Topological Graphs, Reeb Graphs, Graph-based Shape Representation

1 Introduction

While hidden from view, plant roots represent a significant portion of the plant body and are of crucial importance for plant growth and productivity. For phenotyping of roots characteristics such as the number of branches, position of branches, branching angles and the length of roots are analyzed. These characteristics can be captured based on root images and represented using graphs. An important property of root image representations, besides capturing the needed characteristics, is to handle common problems that may occur for the root images, as for example overlaps of roots in the image.

Topological graphs capture branching points and endpoints of roots as nodes in the graph, while the edges in the graphs represent the root's connectivity. Root properties as the number of branches (primary root and lateral roots), length of individual branches or branching angles are therefore obtained as well.

Such topological graphs are for example the medial axis based graphs which were introduced by Blum in [2] (further description by Lee in [10]). Another type of topological graphs are Reeb graphs (for example described by Biasotti et al. in [1]). Topology studies properties of space that are preserved under continuous deformation (these are for example stretching or bending). Therefore, topological properties are for example connectedness and continuity. In comparison, geometry analyzes properties as for example the shape of an object (contour, corners), its size or relative positions. While two shapes may be different regarding geometry (as are for example a square and a circle) these two shapes may be identical regarding topology (here both the square and the circle form one connected component).

For plant phenotyping based on root images a topological analysis of these images possesses advantages over a geometric analysis as roots may transform non-rigidly. Roots may for example bend around an obstacle when growing or they may be rearranged or bended when grown in soil but taken out of the soil for an image. Such actions change the shape of the root and thus its geometric properties. In contrast the roots' connectedness and branching structure, thus its topological properties, are not affected by these actions. Due to this invariance of the topological characteristics to actions as rearranging of roots or bending around an obstacle, these properties provide a stable representation of root images. Such a representation allows for comparison of roots on different days of growth or of different plants on the same day. The approach presented in this paper utilizes these advantages and is therefore based on a topological image analysis and representation.

A medial axis based graph representation is a common representation of root images based on topological graphs. Leitner et al. for example show an analysis of root systems based on a medial axis approach [11]. Galkovskiy et al. as well rely on a medial axis approach to derive a root skeletonization [6]. Iyer-Pascuzzi et al. use the medial axis to compute root lengths [8].

However, this paper presents an automatic image analysis based on Reeb graphs. A first attempt to use Reeb graphs to represent root structures was presented in [9]. Within the scope of this paper, we show that the properties needed in plant phenotyping (length and angles of branches, numbers of branches, etc.) are captured using a Reeb graph based representation of root images. Furthermore, we show that, compared to a medial axis, Reeb graphs possess the ability of solving the problem of overlaps of lateral roots of one plant without additional post-processing. Using a Reeb graph such overlaps can be detected and resolved immediately. Reeb graphs therefore not only provide a simple solution to the problem of overlapping branches but they first of all provide a representation of root images that captures the characteristics needed in plant phenotyping, while at the same time being invariant to continuous deformations and handling the problem of overlaps.

This paper is structured as follows: the dataset as well as the analyzed properties are presented in Section 2. A theoretical introduction to Reeb graphs is given

in Section 3 and the actual approach is described in Section 4, while Section 5 discusses the results. Section 6 concludes the paper.

2 Dataset

For this dataset roots of the plant *Arabidopsis thaliana*, a model organism in plant sciences [7], were grown and imaged on day 7 and day 10 of their growth period.

The plants were grown on a plate of 0.2 Murashige and Skoog (MS) basal media (0.2 MS), with 1% sucrose as a carbon source and pH=5.7 for 7 days. Each plate holds 20 plants, five seeds for any of the four genotypes: Columbia (Col-0), Landsberg erecta(Ler-1), Fei-0 and Bch-1. An example image of such a plate is shown in Figure 1.

After these 7 days of growth, the roots were transferred to plates with a medium of different hormone treatments and were imaged on the following three days. The following hormone treatments were tested: 3-Indolacetic acid (auxin, IAA), Kinetin (cytokinin, CK), Absciscic acid (ABA) and IAA and CK combined. A similar dataset setup is for example described by Ristova et al. in [12].

The approach presented in this paper was evaluated on 66 plants on day 7 and day 10 (132 root images) out of a dataset of 160 plants (320 root images).

On the dataset the following measurements were performed and are available as ground truth: primary root length on the transfer day, day7 (P1); primary root length growth after three days from the transfer day, day 10 (P2); lateral root numbers in day 10 (LR#), length of primary root between first and last lateral root for the day 10 (R) and average lateral root length for the day 10 (LRL), and



Fig. 1: Dataset example image: *Arabidopsis thaliana* roots on day 10, under IAA treatment.

primary root length on day 10 (P).

The ground truth measurements were obtained using Fiji (Image J) by drawing on the original images and extracting the length values.

3 Reeb Graphs and Related Morse Theory

The analysis of the presented dataset is based on Reeb graphs. These graphs are named after the French mathematician Georg Reeb and are based in Morse theory [3]. Reeb graphs describe the topological structure of a shape (e.g. 2D or 3D content) as the connectivity of its level sets [5]. A shape is analyzed according to a Morse function to derive a Reeb graph. Two common Morse functions were tested and used for our data:

- Height Function:

The height function in 2D is defined as the function f that associates for each point $p = (a, b)$ of a function $f(x, y)$ the value b as the height of this point p : $f(x, y) \mapsto y$.

- Geodesic Distance:

The geodesic distance is defined as the shortest distance in a curved space or a restricted area measured between two points of this area or space.

A comparison of the function values generated by these two Morse functions is shown in Figure 2. Figure 2a shows the input image, the Morse function values are shown in Figure 2b for the height function and respectively Figure 2c for the geodesic distance. Here the function values vary strongly for these two Morse functions. However, for a shape, for which changes in topology appear in a mainly vertical direction, both height function and geodesic distance (with the source pixel set in the topmost pixel line) will result in similar function values.

The nodes of a Reeb graph correspond to critical points computed on a shape ac-

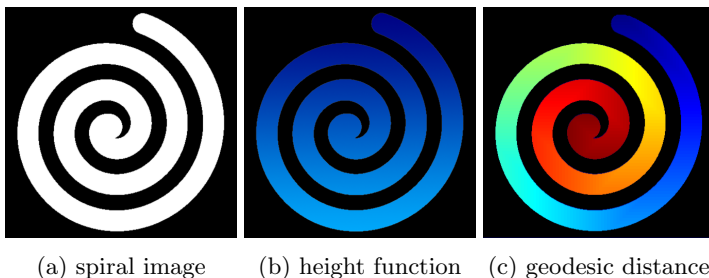


Fig. 2: Example images for the two Morse functions: the height function is computed top-down, the seed point for the geodesic distance is in the center of the topmost pixel line of the foreground. Red indicates high function values, blue low function values.

ording to a Morse function. At critical points the topology of the analyzed shape changes, thus the number of connected components in the level-set changes. At regular points the topology remains unchanged. Edges connecting critical points describe topological persistence.

A point (a, b) of a function $f(x, y)$ is called a *critical point* if both derivatives $f_x(a, b)$ and $f_y(a, b)$ are equal 0 or if one of these partial derivatives does not exist. Such a critical point p is called degenerate if the determinant of the Hessian matrix at that point is zero, otherwise it is called non-degenerate (or Morse) critical point [14].

According to Morse theory Reeb graphs are defined in the continuous domain as follows:

A smooth, real-valued function $f : M \rightarrow \mathbb{R}$ is called a Morse function if it satisfies the following conditions for a manifold M with or without boundary:

- *M1*: all critical points of f are non-degenerate and lie inside M ,
- *M2*: all critical points of f restricted to the boundary of M are non-degenerate,
- *M3*: for all pairs of distinct critical points p and q , $f(p) \neq f(q)$ must hold [4].

Although originally defined for the continuous domain, Reeb graphs have been extended to the discrete domain. For the definition of a discrete Reeb graph, we need to define connective point sets and level-set curves first:

- Two point sets are connected if there exists a pair of points (one point of each point set) with a distance between these two points below a fixed threshold.

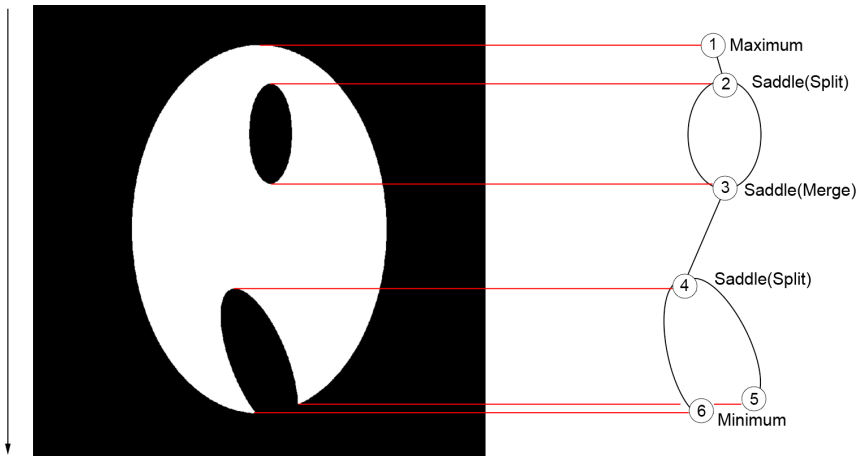


Fig. 3: Reeb graph according to height function and the geodesic distance (here they generate identical critical points), computed for the white foreground region.

- If all non-empty subsets of a point set, as well as its complements, are connected, such a point set is called *connective*.
- A group of points that have the same Morse function value and that form a connective point set, is called a *level-set curve* [16].

The nodes in a discrete Reeb graph represent level-set curves, the edges connect two adjacent level-set curves, therefore the underlying point sets are connected [16].

In 2D three types of nodes in a Reeb graph correspond to critical points: minima, maxima or saddles [4]. We will further distinguish saddle nodes of type split (increase in the number of connected components) and merge (reduction in the number of connected components). Minimum and maximum nodes are of degree 1 (one adjacent node in the graph), saddle nodes are of degree 3 (3 adjacent nodes in the graph). An example Reeb graph containing all possible types of nodes is shown in Figure 3. The nodes in this graph correspond to the critical points of two Morse functions: the height function as well as the geodesic distance both result in this set of nodes.

4 Reeb Graphs in Plant Phenotyping

The methods presented in this section requires a pre-segmented image as an input. Therefore an image segmentation is done as a first pre-processing step. The segmentation is based on the approach presented by Slovak et al. [13]. The transition between shoots and roots is found based on the color information.

The Reeb graphs are computed for the segmented images based on the geodesic distance inside the region of the root (foreground). For each foreground pixel the distance to one predefined source pixel is computed as the chessboard distance. This source pixel is located at the transition between shoots and roots, therefore at the top of the root. Thus, there is only one node of type maximum in a Reeb graph based on the geodesic distance which is the source pixel. Minimum nodes (root tips) are found as the position of a maximal geodesic distance in a branch (local maxima). Saddle points are determined as locations at which foreground parts with the same geodesic distance to the source pixel are split in two connected components or are merged from two into one connected component.

The so found nodes are connected in the Reeb graph according to the root region. For the root dataset evaluated in this paper, a modified approach was used to connect the nodes. Due to noise introduced by the image segmentation the roots of this dataset show a high number of nodes (for example 56 nodes for the root in Figure 6). As in this dataset we only deal with primary roots and lateral roots that do not further branch, we can modify the Reeb graph computation as described in Algorithm 1.

For two nodes (accordingly two critical points) at the same distance (the same Morse function value) a unique Reeb graph cannot be built as this configuration contradicts condition three of the conditions of Morse functions (condition $M3$ in Section 3). Therefore for two nodes at the same geodesic distance (chessboard distance) a second distance measurement, the Euclidean distance is used for the

Algorithm 1 Reeb graph computation

```

connect maximum node to the split saddle node of the smallest geodesic distance
for each split saddle node do
  look for closest split node in each branch  $(s_1, s_2)$ ;
  look for most distant minimum node in each branch  $(m_1, m_2)$ ;
  if  $m_1 < m_2$  then
    connect current split saddle node  $s_c$  to  $m_1$  and  $s_2$ .
    if distance between  $s_c$  and  $m_1 < 10$  pixel then
      discard connection again.
    end if
  else
    connect current split saddle node  $s_c$  to  $m_2$  and  $s_1$ .
    if distance between  $s_c$  and  $m_2 < 10$  pixel then
      discard connection again.
    end if
  end if
end for

```

decision.

The approach described in Algorithm 1 results in a graph for which every minimum node (root tips) represents the end point of a lateral root, respectively the primary root and every saddle node of type split represents the start point of a

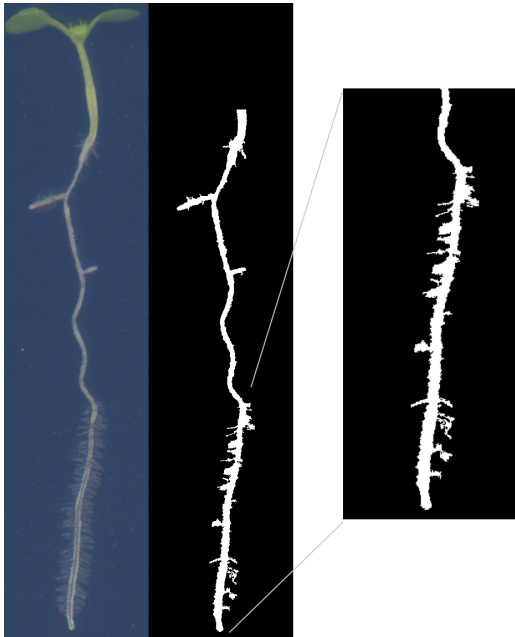


Fig. 4: Segmentation artefacts due to root hairs

lateral root. The maximum node represents the start point of the root. Based on a such a Reeb graph the measurements described in Section 2 can be done based on the geodesic distance values of the individual nodes. The segmentation that is done as pre-processing step introduces artefacts as for example frayed borders (see Figure 4). For these artefacts spurious branches (additional lateral roots) may be added to the graph. Therefore a simple graph pruning is used and branches that are shorter than 10 pixels are discarded. This length was determined empirically to minimize the number of discarded true branches (false negatives) as well as the number of accepted false branches (false positives). An example for such a Reeb graph computed on a root image is shown in Figure 6 in Section 5.

The Reeb graph based approach as presented above provides some advantages when compared to a medial axis based representation:

– Detection of Overlaps:

Due to the projection of the 3D root shape to a 2D image, roots of one plant may overlap in the image. In a graph such an overlap introduces a cycle. For a cycle in the graph a saddle node of type merge is introduced in the Reeb graph (see node number 3 in Figure 3). Based on this particular node, the overlap can be automatically detected in a Reeb graph. To resolve such an overlap, the merge node can be doubled and each node can be connected to one of the adjacent nodes at higher distances. For correct connections the continuity of the direction of growth of a root can be considered. Figure 5 shows an example image (from a different dataset) for such an overlap, the

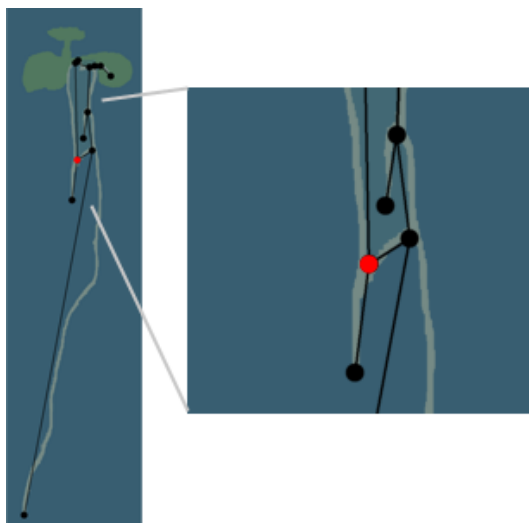


Fig. 5: An overlap of branches in the root image introduces a cycle in the graph and therefore a merge node (highlighted in red) in a Reeb graph.

merge node is highlighted in red.

For a medial axis based graph an overlap is not detected automatically. It may be found looking for cycles in the graph. Since the medial axis has no explicit start point of the root, there is no order induced by distances from the start point. Consequently the crossing of two root branches cannot be resolved as simple as in the Reeb graph.

– Length Measurement:

For a Reeb graph based on a geodesic distance with the source pixel located at the transition between shoots and roots, the geodesic distance provides an implicit measurement of length. The geodesic distance for an endpoint of a root (a minimum node in the Reeb graph) correlates with the length (in pixels) between the source point and this endpoint. Therefore the length between the top of the root and a tip of the root can be easily measured. In the same way the length of lateral roots can be measured as the length between the corresponding saddle node (branching point) and the minimum node (tip of root) which is the difference of their distances to the source pixel.

Such a measurement is not implicitly given by a medial axis based representation, but needs to be computed based on the skeleton. Here the length can be obtained as the number of skeleton pixels between two nodes. A weighted approach (as for example discussed in [15]) that considers different weights for 4- and 8-connected pixels may further be used for a better approximation of the actual root length.

– Analysis of Root Structure:

Due to the different types of nodes in a Reeb graph, numbers of lateral roots can be counted simply as the number of minimum nodes in the graph. Furthermore locations of branches can be easily found as they are represented by saddle nodes of type split.

5 Results on the Dataset

For the evaluation of the approach introduced in Section 4 the method presented is tested on the dataset described in Section 2. For this data ground truth measurements are available and are compared with the results obtained by the Reeb graphs. A subset of 66 of the 160 plants in the dataset was used for the evaluation. For the rest of the dataset the image segmentation was either not available or the quality of the segmentation was too low (for example the primary root was not segmented as foreground in the segmentation image). Therefore these images could not be used in the evaluation of the presented approach.

Figure 6 shows an example for a Reeb graph computed on a root image of the dataset. The branching points indicating the branching positions of lateral roots as well as the tips of the individual roots are represented by nodes in the graph while the edges represent the root structure. According to the ground truth this



Fig. 6: Resulting Reeb graph for root 29_06 on day 10.

root has eight lateral roots, the Reeb graph based approach detects six lateral roots only, as the two additional roots are too short. Therefore they are discarded as spurious branches.

The number of lateral roots can be determined based on the number of nodes representing branching points or on the number of nodes representing root tips. For the Reeb graph based on the geodesic distance measurements of length can be computed directly on the Morse function value as the geodesic distance with the source pixel set to the start of the root (at the transition between roots and shoots) measures the distance inside the root region to this source pixel. This distance corresponds to the intrinsic length in pixel between the top of the root and any position along the root. When measuring the length of roots one possible option is to measure the Euclidean distance between the start point of the root (top of root or branching point for lateral roots) and the endpoint of the root (tip of the root). However, for the Euclidean distance curvature of the root is not taken into account. For the geodesic distance the length is measure inside the root region, and curvature is included in the length. Therefore the geodesic

Table 1: Comparison of average measurements according to ground truth and to Reeb graphs for the subset of 66 plants of the dataset described in Section 2. The mean deviation of the Reeb graph measurements from the ground truth is shown as well. The abbreviations of the measured characteristics are described in Section 2.

Comparison of Measurements - Dataset			
Characteristic	Average Ground Truth	Average Reeb Graph	Mean Deviation from GT
P1 in mm	17.0416	17.2670	0.6893
P in mm	21.7741	23.0805	1.8149
LR#	7 (7.4545)	7 (7.3333)	2 (1.7880)
R in mm	11.2849	12.4798	2.6220
LRI in mm	0.8631	0.6582	0.2902

distance measurement approximates the actual root length better.

For the root images of the dataset evaluated in this paper, a ruler was imaged with the plants to use as a reference measurement. Therefore the computed geodesic distances in pixels were converted to millimeters to compare them to the ground truth measurements.

Table 1 shows an overview of the Reeb graph based measurements compared to the ground truth. While Table 2 shows detailed results for a selection of eight root images of the dataset and the corresponding ground truth. The measurements shown in these tables are:

- **P1**: length of primary root on day 7
- **P**: length of primary root on day 10
- **LR#**: number of lateral roots on day 10
- **R**: length of primary root between first and last lateral root on day 10
- **LRI**: average length of lateral roots on day 10

In general, the length measured for the primary roots according to the Reeb graphs is longer than the ground truth length. The ground truth measurements were done manually by drawing on the root image, while the Reeb graph measurements are based on the geodesic distance (from an automatically detected start point) measured on a segmented image. Differences in the measured length may therefore arise due to the position of the automatically (based on color information) detected start point and due to the image segmentation. The average length measurements for the set of 66 plant images in Table 1 show that the Reeb graph based measurements approximate the ground truth measurements for day 7 well (difference of 0,23mm). The difference in the measurements for day 10 is larger (difference of 1,31mm). As the length according to the Reeb graph representation is measured as the geodesic distance between the top of the root and the tip of the root, curvature is taken into account by this measurement. The roots on day 7 grow in a mainly vertical direction. The older roots on day 10 show more deviation from the vertical direction of growth, they are more

Table 2: Comparison of individual measurements according to ground truth and to Reeb graphs for eight plants of the dataset described in Section 2.

Comparison of Measurements - Individual Plants						
Root	Type	P1 in mm	P in mm	LR#	R in mm	LRI in mm
29_04	GT	17.6445	18.0255	9	15.0199	0.4929
	RG	17.8814	18.0297	5	10.9534	0.3771
29_05	GT	17.6670	18.1525	9	16.9672	0.6830
	RG	18.2839	18.6017	8	16.6525	0.4396
29_06	GT	11.7433	11.5993	8	10.9051	0.8901
	RG	12.8602	12.5000	6	10.4873	0.7521
29_07	GT	12.8270	13.0810	9	12.4460	0.6670
	RG	12.2034	13.3729	8	11.2288	0.6674
29_11	GT	20.3030	21.0058	10	18.6270	0.7612
	RG	20.8475	23.1992	8	14.9364	0.5826
29_14	GT	17.1027	17.7546	9	14.2071	0.8852
	RG	18.4958	18.6017	8	14.6186	0.5244
29_19	GT	21.5053	21.8101	14	18.3642	0.5056
	RG	21.3347	20.0847	11	15.2331	0.5104
29_20	GT	27.4320	27.3558	15	21.8863	0.5904
	RG	26.5890	25.6992	10	17.0339	0.4788

likely to bend. As this length due to bending is directly captured by the geodesic distance, the lengths obtained by this measurement are in general longer.

While the automatically measured lengths of the primary roots match the ground truth well, the other characteristics such as the number of lateral roots or the average length of the lateral roots vary from ground truth to Reeb graph measurements. This difference in the measurements is based on the pre-processing steps needed for the automatic Reeb graph analysis. The ground truth measurements were done on the original root image, while the Reeb graph measurements were done on a segmented image. Lateral roots may be missing in this segmentation, just as segmentation artefacts may be classified as lateral roots. Especially root hairs introduce segmentation artefacts, that resemble small lateral roots and that may be mistaken as roots in the Reeb graph approach. Because of segmentation artefacts, a graph pruning approach was applied to discard small spurious branches. True lateral roots may be discarded by this procedure in case they resemble spurious branches (length shorter than 10 pixels).

Table 2 shows detailed individual results for eight plants to provide a direct comparison of ground truth and Reeb graph based measurements. For each of the four genotypes in the dataset two plants were selected for this subset and all eight plants were grown on the same plate (with IAA and CK treatment). Plant 04 and 05 are of type Bch-1, plant 06 and 07 of type Fei-0, plant 11 and 14 are of type Col-0 and plant 19 and 20 are of type Lan.

In case a shorter length is measured for the primary root on day 10 compared to day 7 (as it is for example the case for plant 20 in Table 2), this is a measurement

error, due to differently detected start points of the roots on these two days. As shown for the overall results of the dataset, the length measurements for the primary roots based on the Reeb graphs approximate the human ground truth. The number of lateral roots in the ground truth and the Reeb graph representations differ for all of these eight plants. This is caused by the image segmentation and graph pruning needed for the Reeb graph based approach.

6 Conclusion

The approach presented in this paper builds a Reeb graph representation based on the geodesic distance for a pre-segmented root image. Measurements regarding lengths or numbers of roots can be derived directly from the graph. Which is not as easily possible for a medial axis approach, as distances between nodes are not stored as function values in a medial axis representation. Another advantage of Reeb graphs is the automatic detection of overlapping branches in the root image, as such an overlap introduces a cycle in the graph and therefore a particular node in a Reeb graph.

However, a Reeb graph representation, as well as a medial axis representation uses a segmented image as its input. The segmentation that is done as a pre-processing step is on the one hand likely to introduce noise and artefacts which may be represented as root structure in the graphs. On the other hand actual parts of the root may be lost during the segmentation process. The quality of a graph representation based on a segmented image depends on the segmentation. Reeb graphs just as well as medial axis representations need a segmentation that does not introduce noise and segmentation artefacts as frayed borders, that resemble small branches of the roots.

Graph representations are suitable for branching structures as roots. Especially Reeb graphs are able to capture the characteristics needed for phenotyping of plants. However the true bottleneck of such an approach is the segmentation. The graph representation can only provide reliable results for a correct segmentation.

Acknowledgements: We thank the anonymous reviewers for their constructive comments.

References

1. Biasotti, S., Giorgi, D., Spagnuolo, M., Falcidieno, B.: Reeb graphs for shape analysis and applications. *Theoretical Computer Science* 392(1-3), 5–22 (Feb 2008)
2. Blum, H.: A Transformation for Extracting New Descriptors of Shape. In: Wathen-Dunn, W. (ed.) *Models for the Perception of Speech and Visual Form*, pp. 362–380. MIT Press, Cambridge (1967)
3. Bott, R.: Lectures on Morse theory, old and new. *Bulletin of the American Mathematical Society* 7(2), 331–358 (1982)
4. Doraiswamy, H., Natarajan, V.: Efficient algorithms for computing Reeb graphs. *Computational Geometry* 42(6-7), 606–616 (Aug 2009)
5. EL Khoury, R., Vandeborre, J.P., Daoudi, M.: 3D mesh Reeb graph computation using commute-time and diffusion distances. In: *Proceedings SPIE: Three-Dimensional Image Processing (3DIP) and Applications II*. vol. 8290, pp. 82900H–82900H–10 (2012)
6. Galkovskyi, T., Mileyko, Y., Bucksch, A., Moore, B., Symonova, O., Price, C., Topp, C., Iyer-Pascuzzi, A., Zurek, P., Fang, S., Harer, J., Benfey, P., Weitz, J.: GiA roots: software for the high throughput analysis of plant root system architecture. *BMC Plant Biology* 12(1), 116 (2012)
7. Hayashi, M., Nishimura, M.: Arabidopsis thaliana - a model organism to study plant peroxisomes. *Biochimica et Biophysica Acta (BBA) - Molecular Cell Research* 1763(12), 1382–1391 (Dec 2006)
8. Iyer-Pascuzzi, A.S., Symonova, O., Mileyko, Y., Hao, Y., Belcher, H., Harer, J., Weitz, J.S., Benfey, P.N.: Imaging and analysis platform for automatic phenotyping and trait ranking of plant root systems. *Plant Physiology* 152(3), 1148–1157 (2010)
9. Janusch, I., Kropatsch, W.G., Busch, W.: Reeb graph based examination of root development. In: *Proceedings of the 19th Computer Vision Winter Workshop*. pp. 43–50 (Feb 2014)
10. Lee, D.T.: Medial axis transformation of a planar shape. *Pattern Analysis and Machine Intelligence, IEEE Transactions on PAMI-4*(4), 363–369 (July 1982)
11. Leitner, D., Felderer, B., Vontobel, P., Schnepf, A.: Recovering root system traits using image analysis exemplified by two-dimensional neutron radiography images of lupine. *Plant Physiology* 164(1), 24–35 (2014)
12. Ristova, D., Rosas, U., Krouk, G., Ruffel, S., Birnbaum, K.D., Coruzzi, G.M.: Rootscape: A landmark-based system for rapid screening of root architecture in arabidopsis. *Plant Physiology* 161(3), 1086–1096 (2013)
13. Slovak, R., Göschl, C., Su, X., Shimotani, K., Shiina, T., Busch, W.: A scalable open-source pipeline for large-scale root phenotyping of Arabidopsis. *The Plant Cell Online* (2014)
14. Stewart, J.: *Calculus*. Cengage Learning Emea, 6th edition. international met edn. (Feb 2008)
15. Vossepoel, A., Smeulders, A.: Vector code probability and metrication error in the representation of straight lines of finite length. *Computer Graphics and Image Processing* 20(4), 347–364 (1982)
16. Werghi, N., Xiao, Y., Siebert, J.: A functional-based segmentation of human body scans in arbitrary postures. *IEEE Transactions on Systems, Man, and Cybernetics, Part B: Cybernetics* 36(1), 153–165 (2006)